Spin-dependent kinetics of polaron pairs in organic light-emitting diodes studied by electroluminescence detected magnetic resonance dynamics

C. G. Yang,[1] E. Ehrenfreund,[1,2] F. Wang,[1] T. Drori,[1] and Z. V. Vardeny[1,*]
[1]*Department of Physics, University of Utah, Salt Lake City, Utah 84112, USA*
[2]*Department of Physics, Technion-Israel Institute of Technology, Haifa 32000, Israel*
(Received 9 August 2008; published 12 November 2008)

We describe a method for characterizing the spin-dependent kinetics of polaron pairs (PP) in polymer organic light-emitting diodes (OLEDs) made from a derivative of poly(phenylene-vinylene), using the dynamic response of spin-$\frac{1}{2}$ electroluminescence detected magnetic resonance (ELDMR) compared with the response of the current-detected magnetic resonance (CDMR). We found that at 10 K the in-phase ELDMR and CDMR responses are positive at low microwave modulation frequency f, but both change sign at a frequency f_0 that depends on the microwave power, current density, and device architecture. The similarity between ELDMR and CDMR response dynamics shows that the two phenomena share a common origin. We identify the underlying ELDMR mechanism as due to current-density increase under resonance conditions that is caused by enhanced PP effective recombination in the device, in agreement with a recently proposed model for explaining the magnetoconductivity in OLEDs. Our data are in disagreement with previous models for ELDMR such as polaron-electroluminescence quenching and triplet-polaron interaction. From a model fit to the data that involves both spin singlet and triplet PP dynamics, we obtained their effective recombination and spin-lattice relaxation rates. We found that the spin-lattice relaxation rate in the active layer increases with the current density in the device, showing the importance of spin-spin interaction in OLEDs.

DOI: 10.1103/PhysRevB.78.205312 PACS number(s): 73.61.Ph, 78.55.Kz, 76.70.Hb

I. INTRODUCTION

The viable elementary *interchain* excitations in organic light-emitting diodes (OLEDs) are charged and neutral species. The charge excitations are positive and negative singly-(polaron) and doubly-charged (bipolaron) carriers that contribute to the current density. Whereas the neutral species are polaron pairs (PP) in the singlet (PP_S) and triplet (PP_T) spin configurations that are precursors to singlet and triplet intrachain excitons; the PP_S and PP_T excitations eventually give rise to the device electroluminescence (EL) and electrophosphorescence, respectively.[1,2] The generation, dissociation, and recombination kinetics of PP excitations are all spin dependent, and this leads to substantial magnetic-field effects (MFEs).[3–16] Giant MFEs, such as magnetoconductance and magneto-EL of up to 25% and 50%, respectively,[17] induced by relatively small magnetic fields H of $\sim$50 mT have been recently observed in a variety of OLEDs with nonmagnetic electrodes, based on π-conjugated polymers or small molecules.[3–16] In fact the MFEs in OLED are the highest known magnetic responses in semiconductors and thus have the potential to be used in magnetically controlled optoelectronic devices and magnetic sensors. Due to the weak field involved, it is largely agreed that the MFE in organic diodes originates from H-dependent spin sublevel mixing via the hyperfine interaction,[9,18,19] which is relatively weak in π-conjugated organic semiconductors.[11] Two competing models have been proposed for explaining the spin-mixing mechanism responsible for MFE in OLED: (i) the *exciton* model in which H changes the PP_S/PP_T intersystem conversion rate[9] or the PP_T-polaron quenching[10] and (ii) the *bipolaron* model that relies on spin-dependent formation of doubly charged excitations.[12]

Optically detected magnetic resonance (ODMR) in organics is in fact a MFE that occurs under resonance condition with microwave (MW) radiation, which upon absorption *induces* spin sublevel mixing among the PP spin sublevels.[19] It is thus not surprising that models similar to those used to explain MFE without MW radiation have been also advanced to explain spin-$\frac{1}{2}$ ODMR in the class of organic semiconductors.[19–30] The two ODMR versions in OLED devices, namely, the EL-detected magnetic resonance (ELDMR) and current-detected magnetic resonance (CDMR), may thus clarify the underlying mechanism for the MFE in these devices. The reason is that the spin mixing process among the PP spin sublevels that participate in these two experimental techniques is induced under controlled MW conditions, such as power and modulation frequency. Because ELDMR involves the radiative transition of singlet excitons, then for explaining its response dynamics it is more convenient to treat the participating spin sublevels in terms of PP_S and PP_T that are precursors to intrachain excitons rather than in terms of four unrelated spin sublevels involving parallel and antiparallel spin-aligned pairs.[19] Using this description in ELDMR the PP_S and PP_T populations continuously evolve due to carrier injection from the electrodes and subsequent PP formation, dissociation, and recombination kinetics under MW radiation in resonance. Therefore it is expected that the ELDMR frequency dynamics response would depend on both PP decay rates, namely, γ_S and γ_T, as well as on the spin-lattice relaxation rate γ_{SL} of the participating PP species.[30]

In this work we use cw $g \approx 2$ ELDMR and CDMR modulation frequency dynamics to characterize the spin mixing process of PP in OLED made from 2-methoxy-5-(2′-ethylhexyloxy) phenylene vinylene [MEH-PPV] polymer as the active layer. The $g \approx 2$ ELDMR and CDMR responses were studied at various MW power P, modulation frequency f, and injected current densities J. We found that

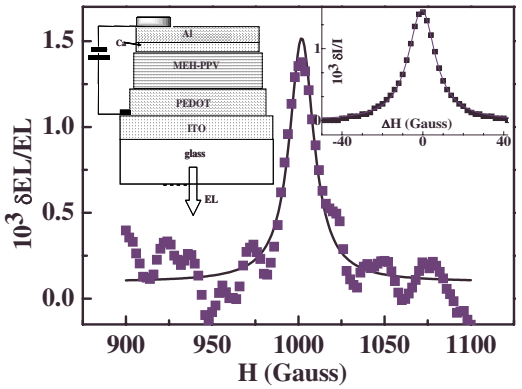

FIG. 1. (Color online) $g\sim 2$ ELDMR resonance vs magnetic field H in an OLED based on MEH-PPV active layer, measured at 10 K and saturated MW power modulated at $f=200$ Hz. The right inset shows the CDMR spectrum at the same g value ($\Delta H=H-H_0$, where H_0 is the peak field), and the left inset shows the device structure composed of ITO anode, hole transport layer (PEDOT/PSS), MEH-PPV active layer, and Ca cathode thin film protected by an Al film.

the in-phase ELDMR and CDMR responses are positive at low f, but both reverse sign at MW modulation frequency f_0 that depends on P, J, and device architecture. From the similarity between the spin-$\frac{1}{2}$ ELDMR and CDMR spectrum, magnitude, and response dynamics we conclude that ELDMR is directly related to the resonantly increased current density in the device, which, in turn is due to enhanced PP effective recombination at resonance conditions. This casts doubts on the triplet-polaron model,[10] as well as the bipolaron model[12] for explaining the narrow positive MFE in organic diodes. From a model fit to the ELDMR response dynamics and its dependence on the MW power we obtained estimates for γ_{SL} and γ for PP_S and PP_T at different current densities. We found that γ_{SL} increases with J, indicating that spin-spin interaction is important in OLED, and this has direct implications on organic spintronics[31,32] and in particular organic spin-valve devices driven at high current density.[33]

II. EXPERIMENTAL

The $g\approx 2$ ELDMR and CDMR measurements were conducted at 10 K using well-balanced OLED devices (shown schematically in Fig. 1 inset) composed of MEH-PPV active layer with thickness of $\sim$100 nm, sandwiched via a hole transport layer poly(3,4-ethylenedioxythiophene) (PEDOT)-poly(styrene sulphonate) (PSS) to an indium tin oxide (ITO) transparent anode on a glass substrate and an evaporated Ca thin-film cathode protected by an aluminum film. The device I-V characteristic and EL-V dependence were measured and showed for all devices a well-balanced OLED with relatively high EL efficiency. The device was mounted in a high Q ($\sim 10^3$) MW cavity; however, due to the metallic electrodes, the cavity Q dropped by a factor of $\sim$10 compared to regular ODMR measurements.[30] The current density J and EL emission were driven at constant bias voltage V, using a Keithley 236 apparatus and their induced changes, $\Delta J(f)$ and $\Delta \mathrm{EL}(f)$, respectively, were measured while subjected to $g\approx 2$ (i.e., at magnetic field $H\sim 0.1$ T) resonance conditions at MW frequency ν of $\sim$3 GHz (S band) that was modulated at frequency f.[6] In-phase ELDMR_I and CDMR_I and quadrature ELDMR_Q and CDMR_Q components with respect to the MW modulation phase were measured at various MW powers and current densities. A background signal that may be due to a thermal effect from the MW absorption by the electrodes was also recorded for both ELDMR and CDMR. This response was not strongly dependent on H or f and thus easily subtracted out from the signal at resonance. In addition, the nonresonant background frequency response could serve as a reference for the response dynamics of the experimental setup.

III. RESULTS AND DISCUSSION

Figure 1 shows $\Delta \mathrm{EL}(H)/\mathrm{EL}$ near the spin-$\frac{1}{2}$ resonance field at $f=200$ Hz. The ELDMR spectrum is composed of a single positive line at $g\approx 2$; no "half-field" resonance at $g\approx 4$ indicative of intrachain triplet excitons involvement was detected. This shows that intrachain triplet excitons do not participate in ELDMR indicating that these species do not participate also in organic MFE in general. This rules out the triplet-polaron model[10] for explaining the magnetoconductivity phenomenon, as well as the polaron-triplet quenching model for explaining the spin-$\frac{1}{2}$ ODMR.[28,29] In Fig. 1 (inset) we show CDMR at $g\approx 2$ resonance condition measured on the same device. $\Delta I(H)$ spectrum also consists of a single positive line of which resonance field, sign, width, and magnitude are the same as those of the spin-$\frac{1}{2}$ ELDMR resonance. The similarity between ELDMR and CDMR resonances indicates that the underlying mechanism for the $g\approx 2$ resonance in the OLED device is shared by these two spectroscopies. This similarity rules out the model of polaron-singlet exciton quenching[25,27] for explaining ELDMR, which states that the decrease in polaron population at resonance eliminates nonradiative centers for singlet excitons and consequently EL increases. In the experiment, however, CDMR is *positive* (Fig. 1), and this shows that the free polaron density *increases* in the device under resonance conditions, in contrast to the proposed model.[25] We thus conclude that the spin sublevels responsible for the $g\approx 2$ ELDMR and CDMR are loosely bound interchain polaron pairs rather than intrachain triplet excitons; more specifically, these are PP_S and PP_T.

We therefore use the following model for explaining the $g\approx 2$ ELDMR and CDMR resonances in OLED. The current density J in such devices is carried out by free charge carriers, but PPs may dissociate into free polarons and thus also indirectly contribute to J.[9,34] The relatively shallow PP_S and PP_T may also form more tightly bound intrachain singlet and triplet excitons, respectively. They may also directly recombine to the ground state by interchain hopping. The *combined effective* PP decay rates that include both dissociation and recombination processes are γ_S and γ_T, respectively, for PP_S and PP_T, where $\gamma_S > \gamma_T$.[21] The PP_S and PP_T steady-state populations n_S and n_T are determined by the respective generation rates $g_T=3g_S$ from the injected free polarons and effective decay rates, where $n_{S,T}=g_{S,T}/\gamma_{S,T}$. Therefore at

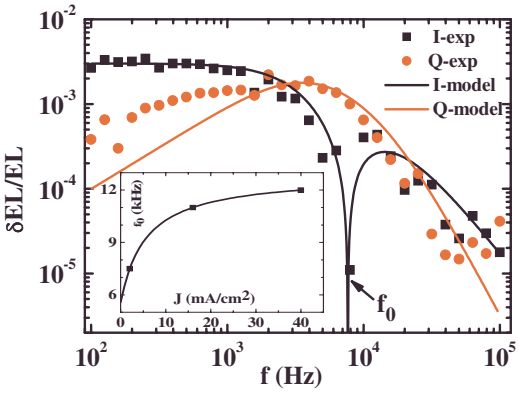

FIG. 2. (Color online) The spin-$\frac{1}{2}$ in-phase (black squares) and quadrature (red circles) ELDMR components in the OLED device shown in Fig. 1, plotted vs the MW modulation frequency f measured at $P_{\mathrm{MW}}=100$ mW and $T=10$ K. "Zero crossing" of the in-phase component occurs at $f_0=7.5$ kHz. The solid lines through the data points are based on a model described in text. The inset shows the dependence of the zero-crossing frequency f_0 vs the device current density J.

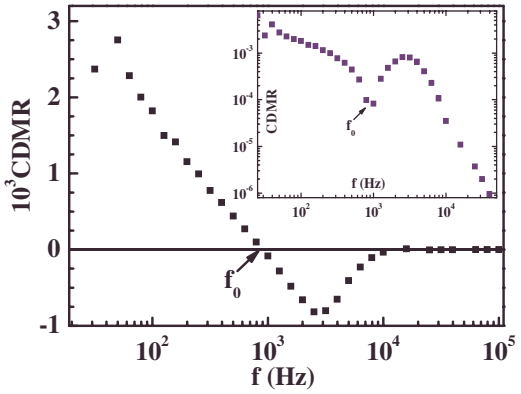

FIG. 3. (Color online) Same as in Fig. 2 but for the spin-$\frac{1}{2}$ CDMR_I (in-phase) component measured on a different device, both in linear and logarithmical (inset) scales.

steady-state current injection with MW off $n_T \gg n_S$. The relatively strong magnetic field H forms three Zeeman splitted spin sublevels in the PP_T manifold, namely, $m_s=1,0,-1$, which are in resonance with the MW photon energy $h\nu$; thus transitions between $m_s=0$ and $m_s=\pm 1$ can be easily induced. The $m_s=0$ sublevel is coupled with the singlet level PP_S via an intersystem conversion rate that is determined mainly by the hyperfine interaction and the difference Δg in the individual g factor of P^+ and P^- in the PP species.[35] Thus any population change in PP_T sublevels has an *indirect effect* on the PP_S population and vice versa. Since $n_T \gg n_S$ in steady state, then the $m_s=0$ PP_T spin sublevel population is relatively small. Consequently the MW transition from the $m_s=\pm 1$ into the $m_s=0$ increases this PP_T spin sublevel population and, in turn, the PP_S population is also enhanced upon resonance. Since $\gamma_S > \gamma_T$ then the MW transition at resonance that increases the PP_S population also increases the overall effective PP recombination rate r in the device, which is due to enhanced direct interchain recombination, formation of intrachain excitons, or both in the PP_S manifold. However the increase in the effective PP recombination rate does not automatically decrease the charge-carrier density in the device since the OLED operates under the condition of *constant applied bias voltage*. In this case the current density in the device adjusts itself to the new condition in the active layer, where r increases. Such a situation was recently described within the exciton model for explaining the positive magnetoconductance obtained in OLED devices.[9,15] In this model the current density in a device operating under high bias voltage in fact increases with r for $r<r_c$, where r_c is a critical recombination rate.[15] Since r increases under resonance condition, then both the current density and consequently also the EL emission increase; this scenario explains the simultaneous positive $g\approx 2$ ELDMR and CDMR resonances. We note that if the dissociation rates would have dominated the two respective γ's, then the current in the device would also increase at resonance; but this would come at the expense of singlet excitons that produce EL and thus would not give positive ELDMR. To distinguish between these two scenarios it is important to resolve the question whether EL at resonance changes as a direct consequence of PP_S population increase[36] or indirectly because of the current increase in the device.[16] The following ELDMR and CDMR dynamics give an unambiguous answer to this question.

Figure 2 shows the measured dynamics of the two ELDMR components at $J=2$ mA/cm^2 and $P=100$ mW. It is seen that the positive ELDMR_I (f) reverses sign at frequency $f_0 \sim 7.5$ kHz before further decaying at higher frequencies; in contrast, ELDMR_Q retains its sign throughout the measured f range. Figure 2 (inset) shows that f_0 increases with J; it increases more sharply at low J and tends to saturate at high J. Similar dynamics response is also typical for CDMR. Figure 3 shows the CDMR dynamics at $J=1$ mA/cm^2; again the positive CDMR_I response at low f reverses sign at high f_0, which increases with J.[37] In addition, we also measured the ELDMR saturation behavior. The MW power dependence of the ELDMR maximum value ($[\mathrm{ELDMR}]_{\mathrm{max}}$) at low f is shown in Fig. 4 at two different current densities; $[\mathrm{ELDMR}]_{\mathrm{max}}$ shows a typical magnetic resonance saturation behavior, from which the relaxation rate and γ_{SL} may be readily obtained (see below and in Ref. 30).

We assume that the ELDMR_I and CDMR_I "zero-crossing" responses are mainly intrinsic in origin, i.e., it is the result of the interplay between the three spin sublevels that are coupled by the MW radiation at resonance; these are $m_s=0$ and $m_s=\pm 1$ PP_T spin sublevels (and consequently also PP_S via intersystem crossing, as discussed above). This type of response dynamics exclusively occurs when *all* spin levels actively participate in determining the measured MFE physical quantity.[30] In our case PP_S effectively decays faster than PP_T, namely, $\gamma_S > \gamma_T$,[19] and thus at steady state when MW is off $n_{S,\mathrm{off}} < n_{T,\mathrm{off}}$.[19] Under resonant MW radiation (MW on) a net transfer from $\mathrm{PP}_T \rightarrow \mathrm{PP}_S$ takes place (via the $m_s=0$ spin sublevel in the PP_T manifold) bringing the system under saturation conditions to a new quasiequilibrium state, where $n_{S,\mathrm{on}}=n_{T,\mathrm{on}}$. This enhances the effective PP recombination and, in turn, leads to the current-density increase.[15] Thus the MW induced change $\Delta n=n_{\mathrm{on}}-n_{\mathrm{off}}$ in the total PP density

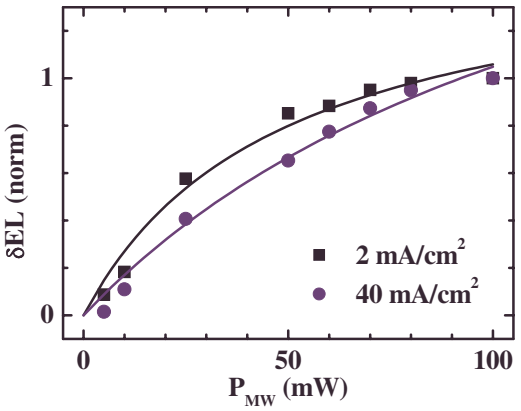

FIG. 4. (Color online) The dependence of spin-$\frac{1}{2}$ ELDMR on the MW power P measured at $f=200$ Hz at two different current densities $J=2$ mA/cm^2 (black squares) and $J=40$ mA/cm^2 (blue circles). Both curves show saturation behavior, where it is harder to reach saturation at larger J.

$n_{PP}=n_S+n_T$ indirectly leads to the current-density increase in the device. Under square-wave MW modulation at high frequency f, both $\Delta n_S(f)$ and $\Delta n_T(f)$ responses decrease (for example, in the form of Lorentzians in f, if their time decays are exponentials[34]); however since $\gamma_T<\gamma_S$, then $\Delta n_T(f)$ response diminishes at a faster rate with f. Also since PP_S population change is positive and PP_T population change is negative, the low-frequency negative $\Delta n(f)$ signal changes sign at a frequency f_0 beyond which it stays positive; this situation is demonstrated in Fig. 5. Therefore any spin-dependent property that is determined by the weighted PP population [such as CDMR (f), for example] would show a sign reversal in its dynamic response. We found that the $g\approx 2$ ELDMR$_I$ and CDMR$_I$ change sign at f_0 (Figs. 2 and 3); we thus conclude that these responses cannot come from change in PP_S population alone (i.e., via singlet formation). On the contrary ELDMR is indirectly determined by the increase in the current density, to which *both* PP_S and PP_T contribute together. This also explains the similarity of the magnetoconductance and magneto-EL responses in the absence of MW resonance conditions.[7]

In order to quantify $\Delta n(f)$ response we make use of the fact that the two triplet spin sublevels ($m_s=\pm 1$) should have a common dynamics. We also take the limit of strong singlet to $m_s=0$ triplet mixing,[30] thus reducing the coupled set of four rate equations to a coupled set of two rate equations for the PP in the triplets and singlet/triplet states, respectively. These equations are written for the experimental conditions $T\gg h\nu/k_B\cong 0.14$ K as follows:

$$dn_i/dt = G - n_i/\tau_i - (n_i - n_j)/2T_{SL} - (n_i - n_j)P, \qquad (1)$$

where $i\neq j=1,2$ denote, respectively, the $m_S=0$ in PP_T and PP_S, and $m_s=\pm 1$ in PP_T, and P is the MW induced spin-flip rate that is proportional to the modulated P_{MW}: $P=\alpha P_{MW}$ ($\alpha\approx 4\times 10^3$ s^{-1}/mW for our experiment). The steady-state solution of Eq. (1) reads

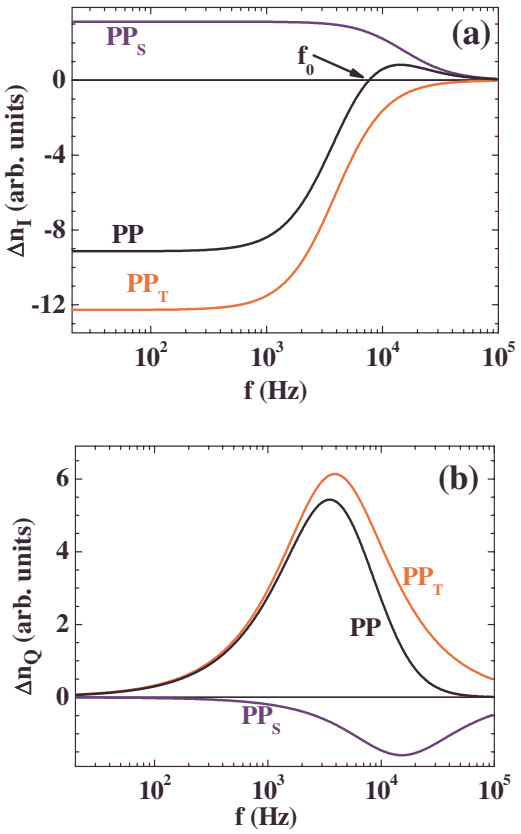

FIG. 5. (Color online) The in-phase (a) and quadrature (b) frequency responses of the change in PP_S (singlet), PP_T (triplet), and the total PP populations based on the solution of Eq. (1) with parameters that fit the spin-$\frac{1}{2}$ ELDMR response shown in Fig. 2. Note the zero crossing of the (a) in-phase component at f_0, which does not occur for the (b) quadrature component.

$$\Delta n/n \equiv [n(P) - n(0)]/n(0) = -[(\gamma_-)^2/\gamma_+\gamma^*]P/(\Gamma_{eff} + P), \qquad (2)$$

where $\gamma_\pm=(\gamma_S\pm\gamma_T)/2$, $\gamma^*=\gamma_+ + \gamma_{SL}$, and

$$\Gamma_{eff} = (\gamma^* - \gamma_-^2/\gamma_+)/2. \qquad (3)$$

Δn thus follows a typical magnetic resonance saturation behavior with an effective rate Γ_{eff} given by Eq. (3) (see Fig. 4). Using the above value of α for our loaded cavity, we obtain from the saturation behavior of Fig. 4 $\Gamma_{eff}=1.9\times 10^4$ s^{-1} for $J=2$ mA/cm^2, whereas at $J=40$ mA/cm^2 $\Gamma_{eff}=5.3\times 10^4$ s^{-1}. This increase in Γ_{eff} is related to the PP density because as J increases, the densities of both free polarons and PP increase. Since the dissociation of PP into free polarons and the formation of deeply bound intrachain excitons are not expected to depend strongly on the PP density, then γ does not change much with J, and thus we are led to conclude that the increase in Γ_{eff} with J is mainly caused by γ_{SL} increase at large J.

We solved equation set (1) with square-wave modulated MW radiation for obtaining the components Δn_I and Δn_Q, as well as $(\Delta n_i)_{I,Q}$ of the individual PP sublevels, as a function of the modulation frequency f. We found that for $\gamma_S>\gamma_T$, $\Delta n_{S,I}(f)>0$ and $\Delta n_{T,I}(f)<0$ for the entire frequency range

(see Fig. 5). However the sum $\Delta n_I(f)$ is *negative* at low f and positive for $f > f_0$, in agreement with the ELDMR$_I$ and CDMR$_I$ results (Figs. 2 and 3). Further analysis of Eq. (1) solution shows that $f_0 \approx (2\gamma_+\Gamma_{\text{eff}})^{1/2}/2\pi$ at low $P(P \ll \gamma_+)$, increasing first linearly with P but tends toward saturation for $P \gg \gamma_+$. Using Γ_{eff} values obtained above from the steady-state saturation measurements, we find from the ELDMR$_I$ zero-crossing frequency f_0: $\gamma_+ = 5.9 \times 10^4$ s^{-1} at $J = 2$ mA/cm^2 and 5.5×10^4 s^{-1} at 40 mA/cm^2. The relatively small change in γ_+ value (i.e., $\sim 10\%$) as J increases by a factor of 20 justifies our conjecture that the main effect on the dynamics due to the current-density increase is increasing γ_{SL}. The extracted values of Γ_{eff} and γ_+ allow us to estimate γ_- and γ_{SL} using Eq. (3). At $J = 2$ mA/cm^2 we obtain $\Gamma_{\text{eff}} < \gamma_+/2$ implying $\gamma_{\text{SL}} < \gamma_-^2/\gamma_+$, and thus $0.6 < \gamma_-/\gamma_+ < 1$ and $\gamma_{\text{SL}}/\gamma_+ < 0.24$. At $J = 40$ mA/cm^2, and assuming that the ratio γ_-/γ_+ does not vary much with J, we obtain from the data $\Gamma_{\text{eff}} > \gamma_+/2$; this implies $\gamma_{\text{SL}} > \gamma_-^2/\gamma_+$ and $\gamma_{\text{SL}}/\gamma_+ > 1.26$. The increase in f_0 with J (Fig. 2, inset) is thus explained as due to an increase in γ_{SL} with the current density. This, in turn, may be caused by an increase in the spin-spin interaction rate in the active layer due to spin-$\frac{1}{2}$ polaron density in the device that increases with J. A similar effect was deduced before when spin-$\frac{1}{2}$ radicals were added to MEH-PPV films.[30] A typical $\Delta n(f)$ response based on the solution of Eq. (1) with $\gamma_S = 9.4 \times 10^4$ s^{-1}, $\gamma_T = 2.4 \times 10^4$ s^{-1}, and $\gamma_{\text{SL}} = 1 \times 10^4$ s^{-1} is shown in Fig. 2, overlaid as a solid line on the experimental data for $J = 2$ mA/cm^2. It is apparent that (i) Δn_I changes sign at f_0 and (ii) Δn_Q does not change sign within the entire f range. The good agreement obtained between the model fit and the data validates the model used.

A necessary condition for the existence of spin-$\frac{1}{2}$ ELDMR and CDMR resonances is that $\gamma_S \neq \gamma_T$.[19] The PP effective decay rates may be decomposed into three different components $\gamma_{S,T} = d_{S,T} + k_{S,T} + r_{S,T}$, where $d_{S,T}$ is the dissociation rate to free polarons, $k_{S,T}$ is the rate at which intrachain strongly bound excitons are formed, and $r_{S,T}$ is the direct recombination rate of PP to the ground state (by direct interchain hopping). Therefore, in addition to ELDMR caused by the change in the overall effective PP recombination rate that leads to an increase in the device current density (as discussed above), a more direct spin-dependent process that also leads to positive spin-$\frac{1}{2}$ ELDMR should also occur;[36] this mechanism is due to enhanced PP$_S$ relative population, where ELDMR $\propto k_S \Delta n_S$. However, since Δn_S alone does not change sign with f (Fig. 5), then the observed zero crossing at finite f_0 leads us to believe that this direct mechanism cannot be the dominant process of the spin-$\frac{1}{2}$ ELDMR, since otherwise ELDMR$_I$ component would not reverse sign at f_0, in contrast with the data. We thus conclude that spin-$\frac{1}{2}$ ELDMR in OLED devices is mainly caused by the current-density increase at resonance, namely, CDMR, rather than MW induced PP$_S$ population increase. This scenario may explain the apparent contradiction in the literature between the similar EL and electrophosphorescence increase intensities in OLED upon application of a strong external magnetic field,[16] as well as the MFE models based on change in PP$_T \rightarrow$ PP$_S$ interconversion rate with H.[9,10,14] In particular we note that the observed positive magneto-EL with H follows the positive component of the MFE in current that is due to increase in the overall effective PP decay rate,[9] rather than the negative MFE component in current, or the overall current change as in Ref. 38. Simply put, the change in relative PP$_S$/PP$_T$ populations with H may not be the *dominant* effect in magneto-EL. On the contrary, the EL increase with H may be directly related to the current-density increase with H from the metallic electrodes.

IV. CONCLUSIONS

In this work we analyzed the spin-$\frac{1}{2}$ ELDMR and CDMR dynamics in MEH-PPV-based OLED devices at various MW power and current density. We found that the in-phase ELDMR and CDMR components reverse sign at finite f_0, thus showing that the increase in EL is caused by a resonant increase in current density (CDMR) in the device, rather than by the direct increase in PP$_S$/PP$_T$ relative population at resonance, or by decrease in polaron density that serves as quenching center for radiative excitons. By analyzing the ELDMR characteristic saturation behavior with the MW power, together with the ELDMR dynamics with f, we obtained the decay rates of PP$_S$ and PP$_T$ polaron pairs, as well as the spin-lattice relaxation rate. Using this model we found that the spin-lattice relaxation rate in the active layer increases with J, probably because of increased spin-spin interaction in the device, with discouraging implications for organic spin valves driven at high current density.[33]

ACKNOWLEDGMENTS

This work was supported in part by the DOE under Grant No. 04-ER 46109, NSF-DMR under Grant No. 08-03172 at the University of Utah, and by the Israel Science Foundation (Contract No. ISF 745/08) at Technion.

*Author to whom correspondence should be addressed.
val@physics.utah.edu

[1] *Primary Photoexcitations in Conjugated Polymers: Molecular Excitons Versus Semiconductor Band Model*, edited by N. S. Sariciftci (World Scientific, Singapore, 1997).
[2] I. Campbell, B. K. Crone, and D. L. Smith, in *Semiconducting Polymers*, edited by G. Hadziioannou and G. G. Maliaras (Wiley, New York, 2007).
[3] I. Kalinowski, M. Coucchi, D. Virgili, P. Dimarco, and V. Fattori, Chem. Phys. Lett. **380**, 710 (2003).
[4] I. Kalinowski, M. Coucchi, D. Virgili, V. Fattori, and P. Dimarco, Phys. Rev. B **70**, 205303 (2004).
[5] A. H. Davis and K. Bussman, J. Vac. Sci. Technol. A **22**, 1885 (2004).

[6] T. L. Francis, O. Mermer, G. Veeraraghavan, and M. Wohlgenannt, New J. Phys. **6**, 185 (2004).
[7] O. Mermer, G. Veeraraghavan, T. L. Francis, Y. Sheng, D. T. Nguyen, M. Wohlgenannt, A. Kohler, M. K. Al-Suti, and M. S. Khan, Phys. Rev. B **72**, 205202 (2005).
[8] Y. Iwasaki, T. Osasa, M. Asahi, M. Matsumura, Y. Sakaguchi, and T. Suzuki, Phys. Rev. B **74**, 195209 (2006).
[9] V. Prigodin, J. Bergeson, D. Lincoln, and A. Epstein, Synth. Met. **156**, 757 (2006).
[10] P. Desai, P. Shakya, T. Kreouzis, W. P. Gillin, N. A. Morley, and M. R. J. Gibbs, Phys. Rev. B **75**, 094423 (2007).
[11] Y. Wu, Z. Xu, B. Hu, and J. Howe, Phys. Rev. B **75**, 035214 (2007).
[12] P. A. Bobbert, T. D. Nguyen, F. W. A. van Oost, B. Koopmans, and M. Wohlgenannt, Phys. Rev. Lett. **99**, 216801 (2007).
[13] F. L. Bloom, W. Wagemans, M. Kemerink, and B. Koopmans, Phys. Rev. Lett. **99**, 257201 (2007).
[14] B. Hu and Y. Wu, Nature Mater. **6**, 985 (2007).
[15] J. D. Bergeson, V. N. Prigodin, D. M. Lincoln, and A. J. Epstein, Phys. Rev. Lett. **100**, 067201 (2008).
[16] M. Reufer, M. J. Walter, P. G. Lagoudakis, A. B. Hummel, J. S. Kolb, H. G. Rosko, U. Scherf, and J. M. Lupton, Nature Mater. **4**, 340 (2005).
[17] T. D. Nguyen, Y. Sheng, J. Rybicki, and M. Wohlgenannt, Phys. Rev. B **77**, 235209 (2008).
[18] T. D. Nguyen, Y. Sheng, and M. Wohlgenannt, Synth. Met. **157**, 930 (2007).
[19] Z. V. Vardeny and X. Wei, *Handbook of Conducting Polymers*, 2nd ed. (Marcel Dekker, New York, 1998), p. 639.
[20] L. S. Swanson, J. Shinar, A. R. Brown, D. D. C. Bradley, R. H. Friend, P. L. Burn, A. Kraft, and A. B. Holmes, Phys. Rev. B **46**, 15072 (1992).
[21] M. Wohlgenannt, K. Tandon, S. Mazumdar, S. Ramasesha, and Z. V. Vardeny, Nature (London) **409**, 494 (2001).
[22] G. B. Silva, L. F. Santos, R. M. Faria, and C. F. O. Graeff, Physica B **308**-310, 1078 (2001).
[23] M. C. Scharber, N. A. Schultz, N. S. Sariciftci, and C. J. Brabec, Phys. Rev. B **67**, 085202 (2003).
[24] F. A. Castro, G. B. Silva, L. F. Santos, R. M. Faria, F. Nuesch, L. Zuppiroli, and C. F. O. Graeff, J. Non-Cryst. Solids **338-340**, 622 (2004).
[25] G. Li, C. H. Kim, P. A. Lane, and J. Shinar, Phys. Rev. B **69**, 165311 (2004).
[26] C. F. O. Graeff, G. B. da Silva, F. Nüesch, and L. Zuppiroli, Eur. Phys. J. E **18**, 21 (2005).
[27] G. Li, J. Shinar, and G. E. Jabbour, Phys. Rev. B **71**, 235211 (2005).
[28] M. Segal, M. A. Baldo, M. K. Lee, J. Shinar, and Z. G. Soos, Phys. Rev. B **71**, 245201 (2005).
[29] C. G. Yang, E. Ehrenfreund, M. Wohlgenannt, and Z. V. Vardeny, Phys. Rev. B **75**, 246201 (2007).
[30] C. G. Yang, E. Ehrenfreund, and Z. V. Vardeny, Phys. Rev. Lett. **99**, 157401 (2007).
[31] W. J. M. Naber, S. Faez, and W. G. van der Wiel, J. Phys. D **40**, R205 (2007).
[32] S. Sanvito, Nature Mater. **6**, 803 (2007).
[33] H. Xiong, D. Wu, Z. V. Vardeny, and J. Shi, Nature (London) **427**, 821 (2004).
[34] D. R. McCamey, H. A. Seipel, S. Y. Paik, M. J. Walter, N. J. Borys, J. M. Lupton, and C. Boehme, Nature Mater. **7**, 723 (2008).
[35] U. E. Steiner and T. Ulrich, Chem. Rev. (Washington, D.C.) **89**, 51 (1989).
[36] M. Wohlgenannt, C. Yang, and Z. V. Vardeny, Phys. Rev. B **66**, 241201(R) (2002).
[37] The zero-crossing frequency f_0 is different in this device compared to that of Fig. 2, and this indicates that the frequency response may also depend on the device architecture.
[38] D. Wu, Z. H. Xiong, X. G. Li, Z. V. Vardeny, and Jing Shi, Phys. Rev. Lett. **95**, 016802 (2005).